The Tendon Network of the Fingers Performs Anatomical Computation at a Macroscopic Scale

Francisco J. Valero-Cuevas*, *Member, IEEE*, Jae-Woong Yi, Daniel Brown, Robert V. McNamara, III, Chandana Paul, *Member, IEEE*, and Hood Lipson, *Member, IEEE*

Abstract—Current thinking attributes information processing for neuromuscular control exclusively to the nervous system. Our cadaveric experiments and computer simulations show, however, that the tendon network of the fingers performs logic computation to preferentially change torque production capabilities. How this tendon network propagates tension to enable manipulation has been debated since the time of Vesalius and DaVinci and remains an unanswered question. We systematically changed the proportion of tension to the tendons of the extensor digitorum versus the two dorsal interosseous muscles of two cadaver fingers and measured the tension delivered to the proximal and distal interphalangeal joints. We find that the distribution of input tensions in the tendon network itself regulates how tensions propagate to the finger joints, acting like the switching function of a logic gate that nonlinearly enables different torque production capabilities. Computer modeling reveals that the deformable structure of the tendon networks is responsible for this phenomenon; and that this switching behavior is an effective evolutionary solution permitting a rich repertoire of finger joint actuation not possible with simpler tendon paths. We conclude that the structural complexity of this tendon network, traditionally oversimplified or ignored, may in fact be critical to understanding brain-body coevolution and neuromuscular control. Moreover, this form of information processing at the macroscopic scale is a new instance of the emerging principle of nonneural "somatic logic" found to perform logic computation such as in cellular networks.

Index Terms—Biomechanical models, complexity, hand, manipulation, model-structure detection, nonlinear systems.

*F. J. Valero-Cuevas is with the Neuromuscular Biomechanics Laboratory, Cornell University, 220 Upson Hall, Ithaca, NY 14853 USA (e-mail: fv24@cornell.edu).

J. W. Yi, D. Brown, and R. V. McNamara, III are with the Neuromuscular Biomechanics Laboratory, Cornell University, 220 Upson Hall, Ithaca, NY 14853 USA.

C. Paul is with the Neuromuscular Biomechanics Laboratory and the Computational Synthesis Laboratory, Sibley School of Mechanical and Aerospace Engineering, Cornell University, 220 Upson Hall, Ithaca, NY 14853 USA.

H. Lipson is with the Computational Synthesis Laboratory, Sibley School of Mechanical and Aerospace Engineering, Cornell University, 220 Upson Hall, Ithaca, NY 14853 USA.
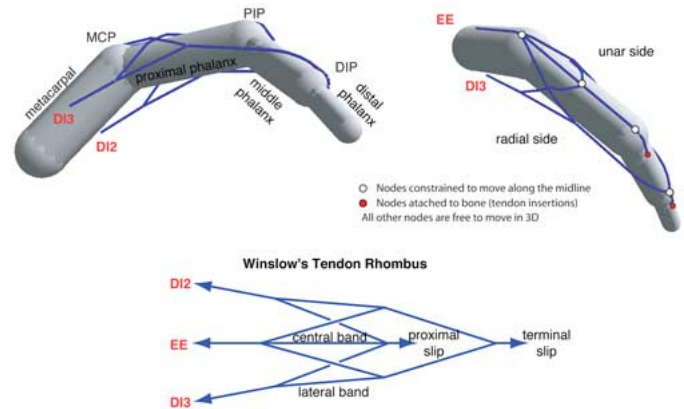
Fig. 1. The tendon network of the middle finger: Winslow's rhombus representation. Most finger muscles actuate the finger joints via a tendon network composed of a sheath of collagen boundless embedded in connective tissue wrapped over the phalanges [8], [9]. Winslow (1669–1760) proposed the tendon network can be approximated by a discrete rhomboidal network of strings [11]. Palmar and dorsal oblique views of a longitudinally symmetric interpretation of Winslow's rhombus, adapted from Zancolli [9], for a 3-D generic right middle finger with the second and third dorsal interosseous muscles (DI2 and DI3, respectively) actuating the lateral inputs, and the extrinsic extensor muscle (EE) actuating the central input. The outputs of the network are the proximal and terminal slips that produce extensor torque at the DIP and PIP, respectively. MCP is the metacarpo-phalangeal joint.

I. INTRODUCTION

INSTANCES of the emerging principle of nonneural "somatic logic" such as intrinsic control [1], cellular circuitry [2], [3], and passive dynamics [4] have been gaining attention and support in recent literature. However, information processing for neuromuscular control is still generally attributed entirely to the nervous system. Muscle coordination for manipulation is an important example of neuromuscular control we do not completely understand even for common finger tasks such as turning this page [5]. Besides its great clinical importance, understanding manipulation lies at the crux of hypotheses about human evolution [6] and the design of versatile robots [7]. Fingers are anatomically remarkable in that their muscles act through a complex tendon network (also called the *extensor mechanism* or *extensor hood*) (Fig. 1). The importance of the tendon network is well documented for healthy and impaired finger [8]. The prevalent thinking among hand anatomists and surgeons about the structure and function of the tendon network [8], [9] remains faithful to early notions that it is a complex network of collagen strings [10], [11]. It was first approximated by Winslow as a longitudinally symmetric tendon rhombus [9], [11] where the posture of the finger and input muscle forces alter the propagation of tension though the network (Fig. 1). In contrast, biomechanical studies of finger neuromuscular control
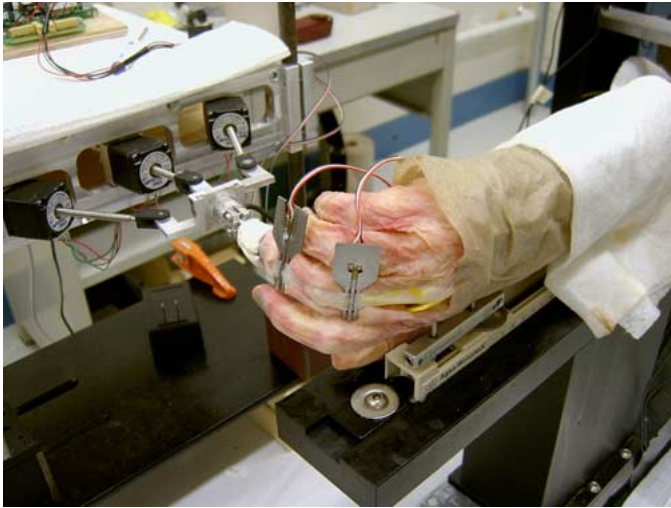
Fig. 2. Experimental apparatus to actuate and measure from the tendon network of the middle finger. Mounted hand with the middle finger set to the standard flexed configuration of 45° flexion at the metacarpophalangeal and proximal interphalangeal joints, and 10° flexion at the distal interphalangeal joints with neutral abduction. The fingertip is rigidly coupled to a six-axis force/torque transducer held by a finger-positioning mechanism. Two buckle transducers were designed and made to measure the tension at the proximal and terminal slips of the tendon network.
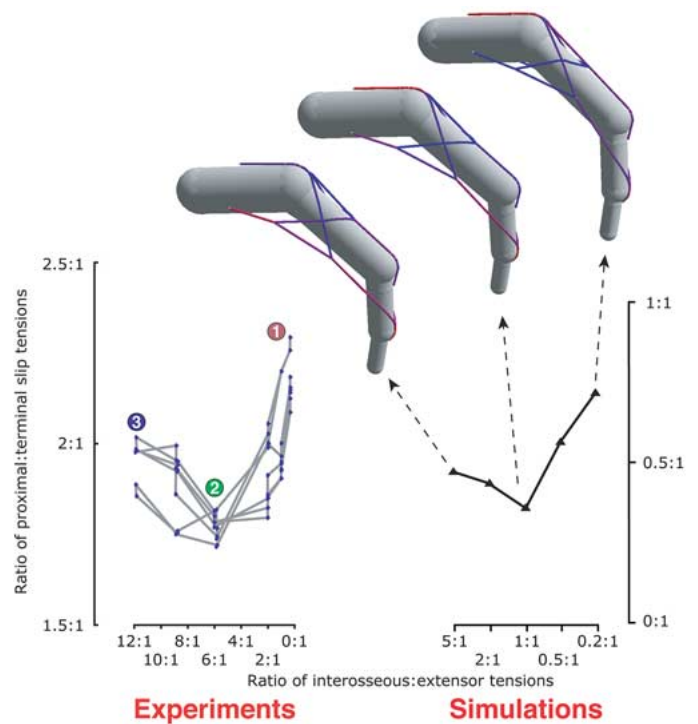

Fig. 3. Switching behavior in the transmission of tension to the distal joints of the finger. (left) Experimental results from one specimen, representative of the two specimens: The distribution of input tensions to the tendon network (abscissa, ratio of interosseous:extensor tensions or $(DI2 + DI3) : EE$) regulates how tensions propagate to the proximal and terminal slips (ordinate, ratio of proximal:terminal slip tensions). The sum of input tensions at DI2, DI3, and EE input tendons was constant at 40 N, but we varied the fraction of tension to the central extrinsic extensor tendon as indicated by the ratio of interosseous to extensor tensions (abscissa). The ordinate indicates the dramatic change and reversal in the proportion of output tension reaching the proximal and terminal slips. Raw data for three full cycles of loading are shown, after preconditioning of the specimen. The torque actuation for the three labeled states of the tendon network are shown in Fig. 4. (right) Computational simulation results: A tendon network compatible with Winslow's rhombus shows a qualitatively similar behavior where the induced change in the relative actuation of the proximal and terminal bands is reversed. The control signals (input tendon tensions) can be made to preferentially propagate tension to the proximal and terminal slips by nonlinearly rerouting the propagation of tensions (finger figures with color-coded strings: red high tension; blue low tension). Although the actual tension ratios in the experiment and model differ, the conclusions reached here rely only on the fact that a simulated 3-D tendon network can exhibit this switching behavior, whereas simple tendon paths cannot (see Section IV).

have adopted simpler, computationally tractable versions of this tendon network where tension propagation is an invariant function of the input tendon excursions, or force magnitudes and distributions (e.g., [12]–[16]). While recent work proposes that these simplifications preclude realistic predictions of finger forces and motions [16], [17], the traditional view of musculoskeletal modeling holds that increasing the complexity of the anatomy will necessarily complicate its control. This raises the question of what functional advantages the tendon network of the fingers may provide.

Based on the work of early anatomists [10], [11] and clinical thinking [8], [9] suggesting a context-sensitive function, we hypothesize that the structure of this tendon network enhances neuromuscular function. Specifically, the tendon network actively responds to the distribution of input tensions to re-route the propagation of tensions and achieve a repertoire of joint actuation not possible with simple tendon paths connecting each muscle to one bone. We tested this hypothesis using computer-controlled cadaveric experiments [18] (Fig. 2) and a novel biomechanical modeling environment [19].

II. MATERIALS AND METHODS

A. Cadaveric Actuation and Measurement

As in other cadaveric studies, two fresh cadaveric hands were resected at the mid-forearm and we isolated the insertion tendons of the extrinsic extensor (EE), and second and third dorsal interosseous (DI2 and DI3, respectively) muscles of their middle fingers (Fig. 2). The tendons were glued to braided Nylon strings connected to computer-controlled force actuators that produced the input tensions to each tendon (For details on the protocol and the actuators, see [18]). To avoid damage to the specimens, the maximal input tendon tensions are compatible with 30% of the force generating capacity of these muscles [16], [20]. We configured the middle finger in a standardized flexed posture with 45° of flexion at the

metacarpophalangeal (MCP) and proximal interphalangeal (PIP) joints, and 10° of flexion at the distal interphalangeal (DIP) joint. The middle finger tip interfaced with a rigidly held 6 degree-of-freedom force/torque sensor (F/T nano17, ATI/Industrial Automation, Garner, NC) via a thermoplastic thimble formed around, and glued to, the distal phalanx as done previously [18]. The tension applied to the inputs of the tendon network (i.e., EE, DI2, and DI3, Figs. 1 and 3) were longitudinally symmetric (i.e., $DI2 = DI3$) and balanced such that $EE + DI2 + DI3 = 40$ N. However, we varied the fraction of tension to the central extrinsic extensor in a linear and monotonic way such that the ratio of $(DI2 + DI3) : EE$ varied from zero to 12 [Fig. 3 (left)]. The sequence of tensions was applied in a quasi-static ramp-and-hold manner simultaneously to all tendons: a linear 5 s ramp transitioned between combinations of input tensions; upon reaching the desired tension an electric motor with an off-center rotating mass applied vibrations for

5 s to the assembly guiding the strings pulling on the tendons to remove any stiction; immediately thereafter we recorded data at a 1000 Hz sampling rate for the last 500 ms to conclude the hold phase before ramping to the next set of input tensions. The mean value for the data over that interval is reported. The recorded data was the measurements of tension at the outputs of the tendon network (the proximal and terminal slips of the tendon network) in situ via custom-built tendon buckle transducers with full-bridge strain-gauge wiring (Fig. 2) to find the ratio of proximal:terminal slip tensions [Fig. 3 (left)]. We preconditioned the specimens by applying 10 cycles of loading to stabilize the response of the system. The three full cycles of raw data in Fig. 3 (left) show what we consider a stable response. These stable data and detailed inspection to the specimen at the completion of the study suggest that the testing did not damage the specimens.

B. Computational Environment

We developed a computational environment to describe the structure of arbitrary topological arrangements of building blocks representing tendons (elastic strings) and bones (stiff rods). For details, see [21]–[23]. The model is a quasi-static forward simulation process that uses an iterative relaxation algorithm similar to that used for design automation of robotic neuro-musculo-skeletal structures, such as the tendinous network wrapped over fixed bones, as in this study. We defined sliding nodes as the proximal nodes of the EE, DI, and PI input strings to move in a straight line to simulate the muscles' lines of action. The nodes representing the insertions of the proximal and terminal slips move only to stay collinear with bone endpoints. This relaxation solver is a viable and attractive alternative to finite-element solvers for modeling of fingers because it can take into account large deformations, accommodates highly nonlinear behaviors typical of biomechanical tissue (e.g. a tendon is nonlinearly elastic as it sustains tension but not compression, and is robust in handling singularities in the model (e.g. tendon bifurcations or junctions in the tendon network) and other model instabilities. Thus, it is appropriate to simulate complex and deformable tendon networks.

C. Models of the Finger and Winslow's Rhombus

The topology of the Winslow's rhombus tendon network (i.e., the number and connectivity of strings that compose it) we studied is compatible with our published finger models [16], [20] (Fig. 3). Given that the focus of this work is to investigate the effect of loading on tension propagation through a network of simulated tendons: 1) All elastic strings were assigned the same nominal stiffness of 1 GPa, a realistic value from the literature [24], with a radius of 0.5 mm; 2) the nodes defining the finger joints were fixed in space to define the posture studied. The nodes and rods defining the phalanges had a stiffness of 8 GPa, radii of 10, 8, 6 and 4 mm and lengths of 40, 50, 31, and 20 mm for the metacarpal, proximal, middle, and distal phalanges, respectively; the flexion joint angles were 45°, 45°, and 10° for the MCP, PIP, and DIP, respectively; 3) The bony insertions of DI and EE tendons onto the proximal phalanx were not included because they vary across fingers; 4) the lumbrical muscle was not included because its insertion varies across fingers and, for the purposes of this study, we focused on a longitudinally symmetric network with one input tendon on each side. Passive tissue exists to keep the extensor mechanism

centered on the finger. To emulate the passive fascia aligning the tendon network [8], the two nodes defining the central band were constrained to stay in the sagittal plane. All other nodes were free to move in 3-D (Fig. 1). The maximal simulated applied 40 N force is compatible with 30% of the force generating capacity of the extrinsic extensor and interosseous muscles of the middle finger [8].

D. Graphical Representation for Torque Actuation and Feasible Torque Sets

The set of all possible joint-torque combinations a set of muscles can produce on a finger is effectively described and quantified by the feasible torque set. For a detailed description of how to calculate feasible torque sets please see [5]. The anatomical routing of tendons results in a moment arm at each joint. These moment arms determine the contribution of each muscle force to the torque at each joint, which can be shown graphically as a basis vector in "torque space": the component along each coordinate dimension is the magnitude of the torque that muscle produces at that joint [Fig. 4 (top)]. Note that torque space has three dimensions corresponding to the flexion-extension torque each muscle produces at the MCP, PIP, and DIP joint, which corresponds to control of the finger while maintaining neural ad-abduction. The moment arm ratios at each joint crossed give the direction of the basis vector, and tension in the tendon defines the magnitude of the basis vector. For example, because the flexor superficialis tendon flexes the MCP and PIP joints only, its basis vector for maximal flexor superficialis force lies on the positive MCP-PIP plane as shown in Fig. 4 (top). Flexor moment arms are assumed to produce positive joint torque. The flexor profundus tendon, in contrast, flexes all three joints and its basis vector points into the positive octant of the torque space. The tendon network produces a torque vector whose MCP flexion component is equal to the net sum of flexion torque produce by the intrinsic muscles minus the extensor torque from the extensor muscle. The PIP and DIP components of this basis vector are given by the relative tension at the proximal and terminal bands times their respective moment arms. When several muscles act on the finger, the net torque at all joints is given by the sum of the respective basis vectors scaled by the force produced by each muscle, which is a point in torque space [5]. The feasible torque set is a convex volume in torque space that shows the range of all possible net joint torques. To be able to produce fingertip force in every 3-D direction, the finger should be able to produce net joint torques in all octants of torque space [5]. The feasible torque set is calculated by the convex hull of all possible positive vector additions (i.e., Minkowski sum) of the basis torque vectors [5]. The biomechanical uniqueness and versatility of the tendon network is revealed by the fact that the distribution of input tendon tensions change both the *direction and magnitude* of its basis vector (see torque vectors for states 1, 2, and 3 in Fig. 4, corresponding to those in Fig. 3), which in turn can change the size and shape of the feasible torque set [Fig. 4 (bottom)]. In comparisons, a change in muscle force for tendons with simple paths connecting each muscle to one bone *can only modify the magnitude* of the basis vector—and have feasible torque sets with fixed size and shape. We calculated the basis of torque vectors for the flexion-extension joints of the MCP, PIP, and DIP joints of the middle finger in Fig. 4 by multiplying normalized muscle strengths [8] by moment arms reported in the literature for the index finger [16], which are the best available estimates for those of the middle finger. In this
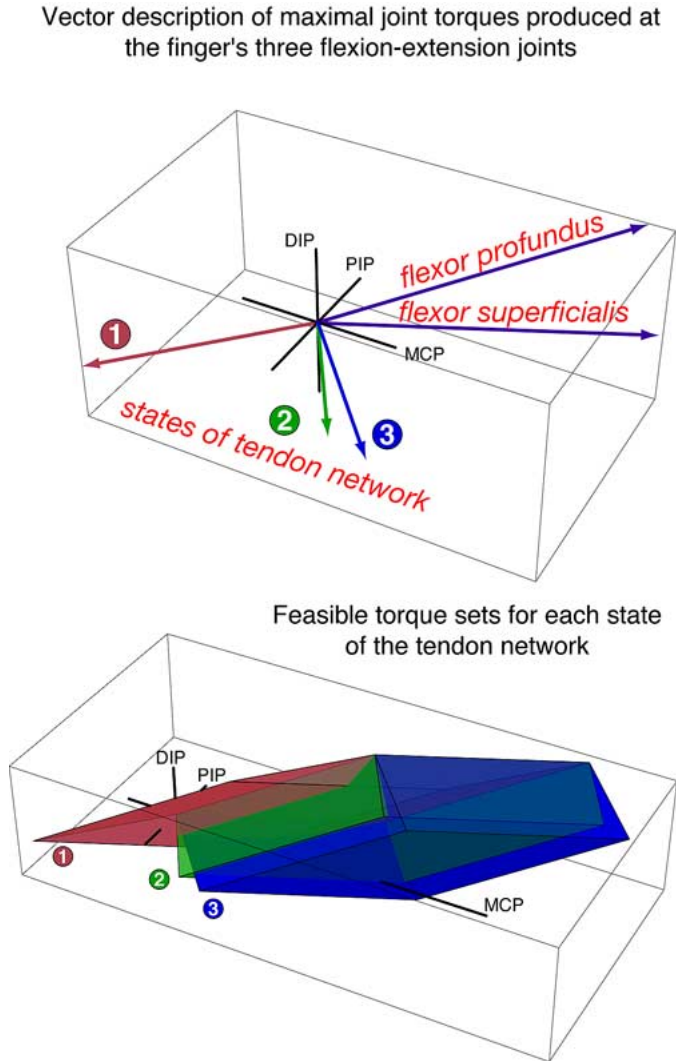
Fig. 4. The tendon network nonlinearly enables different torque production capabilities. Vectors in 3-D "torque space" describe a tendon's contribution to the flexion (positive) and extension (negative) joint torque at the three flexion joints of the finger (MCP, PIP, and DIP; Fig. 1), represented by orthogonal axis [5] (see Section II). We combined the experimental results in Fig. 3 with a published model of the finger to calculate the torque actuation capability of the tendon network and the flexor profundus and flexor superficialis, which have "simple" tendon paths connecting one muscle to one bone (see Section II) (top). The direction of the basis vectors for torque actuation are fixed by the ratio of moment arms at each joint. For the flexors muscles, tendon tension *can only modify torque vector magnitude*. The tendon network is unique in that the distribution of input tendon tensions changes both the torque vector direction and magnitude of torque actuation (see states 1, 2, and 3 corresponding to those in Fig. 3). (bottom) The distribution of input tensions in the tendon network itself regulates how tensions propagate to the finger joints, enabling different torque production capabilities. The feasible torque sets (convex hulls of torque actuation shown as solid volumes, see Section II) quantifies torque production capabilities. Note that the feasible torque sets have different *size and shape* as a result of the anatomical computation in the tendon network. If the finger had simple tendon paths its feasible torque sets would have fixed size and shape.

study, relative torque productions suffices to describe the mechanical consequences of the anatomical gaiting performed by the tendon network.

III. RESULTS

Our results consist of three parts: the results from experimental measurements in cadaver fingers [Fig. 3 (left)], computer simulations of the tendon network [Fig. 3 (right)], and a graphical interpretation of our experimental results showing how the function of the tendon network changes the feasible torque production of the finger (Fig. 4).

Our experimental results show that monotonically changing in the distribution of input tensions reaches a point where the induced change the relative actuation of the proximal and terminal bands is reversed, analogous to the switching function of a logic gate [Fig. 3 (left)]. That is, changing the relative tension distributions to the inputs of the tendon network (the extrinsic extensor, and second and third dorsal interosseous tendons, Fig. 1) changes the distribution of tension in the outputs of the tendon network (the proximal and terminal slips). From a biomechanical perspective, our experimental results show that the ratio of tension in the extensor versus interosseous tendons determines the combinations of extension torque that are produced at the PIP and DIP joints by changing the magnitude of tensions in the proximal versus terminal slips.

In agreement with the experimental results, our computational simulations show that *Winslow's rhombus* (Fig. 1) exhibits the same switching behavior. [Fig. 3 (bottom graph)] shows the predicted tension propagation in *Winslow's rhombus* for five balanced and longitudinally symmetric loading conditions where we varied the distribution of muscle forces across its input tendons (see Section II). We approximated the tendon network as proposed by *Winslow's rhombus* in 1732 [9], [11], and simulated a 3-D tendon network wrapped over simulated rigid bones in the same flexed finger posture as the experiment (see Section II, Figs. 1 and 3). This allowed us to quantify how the propagation of tendon tension changes as function of the distribution of input tensions. Fig. 3 emphasizes the qualitative similarities between the experimental results and computational simulations. However the actual tension ratios in the experiment and model differ substantially. Tuning the model structure and numerous parameters to achieve quantitative agreement is a challenging modeling task we are undertaking, and which is beyond the scope of this work. Our conclusions, however, rely only on the demonstrated fact that a simulated 3-D tendon network based on Winslow's anatomical insight was able to exhibit this switching behavior. A nondeformable net where tension propagation is an invariant function of the input tendon excursions—as most current models of finger anatomy propose [12], [13], [15]—by definition cannot display this behavior.

By using the experimental results to predict torque production capabilities (Fig. 4), we also find that the nervous system and the tendon network work synergistically to preferentially reach different regions of torque actuation. Fig. 4 shows how changing the relative actuation of the proximal and terminal bands changes feasible torque actuation of the finger (regions 1, 2, and 3 in Fig. 4 correspond to the loading conditions in Fig. 3). As described in Section II, the regions of feasible torque actuation were calculated by combining the experimental measurements of propagations of tendon tensions to the distal joints (Fig. 3) with moment arm and muscle cross-sectional area from a published finger model. Changing the relative distribution of tension at the proximal and terminal slips changes the flexion-extension torque at the MCP joint, as well as the extensor torques that can be produced at the PIP and DIP joints. By adding the torque production capabilities of the remaining finger muscles (the flexor profundus and superficialis), we show graphically how the basis vectors for the tendon network change in magnitude and direction [Fig. 4 (top)]. These changes

in torque production capabilities of the tendon network then change the *size and shape* of the feasible torque set, as well as *the octants it can reach* [solid volumes in Fig. 4 (bottom), see Section II]. More specifically, in systems with simple tendon paths that connect one muscle to one bone, the distribution of input tensions (i.e., neural control) can only scale the size of the feasible torque set, but can never change the octants it can reach. Thus, the interconnections of the tendon network provide somatic logic to enable the nervous system to achieve a wider variety of joint actuation than possible with simple tendon paths connecting each muscle to one bone.

IV. Discussion

To our knowledge this is a first example of an anatomical structure capable of information processing and computation normally attributed to the nervous system. The switching of tension distributions and the deformation of the feasible force set made possible by the tendon network is a form of information processing, and a first macroscopic example of the emerging principle of nonneural "somatic logic" known to perform logic computation at various scales, such as cellular circuitry in gene regulation networks [2], [3]. Our findings show than an anatomical structure can, in a manner similar to a switch, synergistically interact with the nervous system to modify the *interpretation* of control signals (i.e., the simulated muscle tensions delivered by linear motors). Specifically, the structure of the tendon network permits the relative activation of subsets of the network to preferentially propagate tension to different joints at a given finger posture. Said differently, the tendon network enables the nonlinear behavior where the distribution of input signals changes the basis vectors for torque production that enable the nervous system to achieve a wide variety of joint torques (i.e., changes in the size and shape of the feasible torque set, Fig. 4 (bottom). Therefore the structure of the tendon network, traditionally oversimplified for the sake of computational tractability, may in fact play a more critical role in understanding neuromuscular control, its impairment and treatment than previously recognized. At least in the case of manipulation, theories of neuromuscular control such as internal models [25] and the organization of muscle synergies [26] need to consider that part of the controller is embedded in the anatomy, contrary to current thinking that attributes the control of human anatomy exclusively to the nervous system.

From a historical perspective, our findings validate early notions [10], [11] about the context-sensitive function of the tendon network of the fingers, and for the first time quantify the ability of Winslow's rhombus to capture this behavior. Because simulations of Winslow's rhombus can reproduce the reversal in relative actuation of the proximal and terminal band (Fig. 3) and change the size and shape of the feasible torque set [Fig. 4 (bottom)], we can confidently conclude that our results validate Winslow's seminal insight in the early 18th century into the function of the tendon network: implementing his simple rhombus topology [9], [11] suffices to capture the major trend in the behavior of this complex system, at least to a first approximation. The reversal in relative actuation of the proximal and terminal bands, and the changes in the size and shape of the feasible torque, set are clear results even for the one possible topology (Figs. 1 and 3) and two cadaveric specimens we present.

This work critically enlarges the debate on brain-body co-evolution [6] and suggests that anatomical features of the human hand may be instrumental to our manipulation ability. Our results highlight the biomechanical uniqueness and versatility of human fingers by showing that the nervous system and tendon network work synergistically to reach different regions of torque actuation [Fig. 4 (bottom)]. One could argue that the degrees-of-freedom of control over the inputs to the tendon network are mathematically equivalent to having muscles whose resultant torque vector have variable magnitude and direction. This, however, is anatomically impossible because fingers do not have muscles that can actuate the PIP and DIP joints in isolation (all finger muscles are multiarticular), emphasizing that the tendon network is an effective evolutionary solution to the problem of versatile finger joint actuation when all muscle must be housed proximal to the MCP joint. We use the term "versatile" in a mechanically rigorous sense that the size, shape and octants covered by the feasible torque set augments the feasible directions and magnitudes of fingertip forces [5]. Thus by allowing the feasible torque set to reach different regions of the toque space [e.g., volumes 1–3 in Fig. 4 (bottom)], the synergistic interaction between the nervous system and tendon network allow the finger to produce fingertip forces of different magnitudes in a variety of 3-D directions. Thus, this shared neural-anatomical control defines the range of fingertip forces that can be produced, and the amount of co-contraction necessary to produce them [5], [16]. In contrast, if finger muscles had simple tendon paths connecting each muscle to one bone it would only be possible to change the size but not the shape of—or octants reached by—the feasible torque set. This first study, therefore, sets the stage for future work to understand why and how the disruption of this network results in dysfunction and/or finger deformities, whether the fingers of other hominids and mammals share similar somatic logic properties, and how to build versatile robotic mechanisms comparable to the human hand.

Future work to refine our tendon network models is necessary to more precisely reproduce experimental values, and will help clarify basic science and clinical questions. Our simplified modeling approach (which is consistent with the computational state-of-the-art for the tendon network) in one finger posture has limitations by virtue of being the first attempt to simulate tension propagation through a complex deformable tendinous network in 3-D. For example, the work presented applies to laterally symmetric control of the finger for it to remain in the sagittal plane, and the range of ratios of input tension over which the model showed the reversal in propagation of tensions to the proximal and terminal slips differed from the range of ratios in the experiments (Fig. 3). We will also need to expand and further validate our results as we refine the stress-strain curves and material properties for simulated collagen strings, and systematically search the large space of model topologies to achieve true quantitative agreement with experimental results (for a detailed discussion of the challenges of simultaneous optimization of model topologies and parameters see [5]). This task by no means only a computational challenge, but also requires further conceptual definition because 1) anatomists still debate the number, orientation and insertion of tendon elements, and we only know of one small-scale study of the material properties of the tendon network [24], [27]; 2) the question of how muscle forces propagate though the tendon network remains controversial because of anatomical variability, the variety of possible interpretations of which tissue is considered load-bearing, and the numerous possible combinations of inputs muscle forces [5], [27], [28]; 3)

the structural and functional complexity of the tendon network challenges even the most experienced anatomist and surgeons to understand and predict how injury, pathology, and treatment affect our ability to move and configure the fingers [8].

ACKNOWLEDGMENT

REFERENCES

[1] F. J. Livesey, T. L. Young, and C. L. Cepko, "An analysis of the gene expression program of mammalian neural progenitor cells," *Proc. Nat. Acad. Sci. USA*, vol. 101, pp. 1374–1379, 2004.

[2] E. Yeger-Lotem, S. Sattath, N. Kashtan, S. Itzkovitz, R. Milo, R. Y. Pinter, U. Alon, and H. Margalit, "Network motifs in integrated cellular networks of transcription-regulation and protein-protein interaction," *Proc. Nat. Acad. Sci. USA*, vol. 101, pp. 5934–5939, 2004.

[3] R. Milo, S. Itzkovitz, N. Kashtan, R. Levitt, S. Shen-Orr, I. Ayzenshtat, M. Sheffer, and U. Alon, "Superfamilies of evolved and designed networks," *Science*, vol. 303, pp. 1538–15342, 2004.

[4] S. Collins, A. Ruina, R. Tedrake, and M. Wisse, "Efficient bipedal robots based on passive-dynamic walkers," *Science*, vol. 307, pp. 1082–1085, 2005.

[5] F. J. Valero-Cuevas, "An integrative approach to the biomechanical function and neuromuscular control of the fingers," *J Biomech*, vol. 38, pp. 673–684, 2005.

[6] F. R. Wilson, *The hand: How Its Use Shapes the Brain, Language, and Human Culture*, 1st ed.   New York: Pantheon Books, 1998.

[7] R. M. Murray, Z. Li, and S. S. Sastry, *A Mathematical Introduction to Robotic Manipulation*.   Boca Raton, FL: CRC Press, 1994.

[8] P. Brand and A. Hollister, *Clinical Mechanics of the Hand*, 3rd ed.   St. Louis, MO: Mosby-Year Book, 1999.

[9] E. Zancolli, *Structural and Dynamic Bases of Hand Surgery*, 2nd ed. Philadelphia, PA: Lippincott, 1979.

[10] A. Vesalius, *De Humani Corporis Fabrica Libri Septem*.   Basileae: Ex officina I. Oporini, 1543.

[11] J. B. Winslow, *Exposition Anatomique de la Structure du corps Humain*.   Paris, France: Chez Guillaume Desprez et Jean Desessartz, 1732.

[12] K. N. An, E. Y. Chao, W. P. Cooney, and R. L. Linscheid, "Normative model of human hand for biomechanical analysis," *J. Biomech.*, vol. 12, pp. 775–788, 1979.

[13] C. W. Spoor, "Balancing a force on the fingertip of a two dimensional finger model without intrinsic muscles," *J. Biomech.*, vol. 16, pp. 497–504, 1983.

[14] E. Y. Chao, J. D. Opgrande, and F. E. Axmear, "Three dimensional force analysis of finger joints in selected isometric hand functions," *J. Biomech.*, vol. 19, pp. 387–396, 1976.

[15] J. N. Leijnse, J. E. Bonte, J. M. Landsmeer, J. J. Kalker, J. C. Van der Meulen, and C. J. Snijders, "Biomechanics of the finger with anatomical restrictions—The significance for the exercising hand of the musician," *J. Biomech.*, vol. 25, pp. 1253–1264, 1992.

[16] F. J. Valero-Cuevas, F. E. Zajac, and C. G. Burgar, "Large index-fingertip forces are produced by subject-independent patterns of muscle excitation.," *J. Biomech.*, vol. 31, pp. 693–703, 1998.

[17] J. L. Sancho-Bru, A. Perez-Gonzalez, M. Vergara-Monedero, and D. Giurintano, "A 3-D dynamic model of human finger for studying free movements," *J. Biomech.*, vol. 34, pp. 1491–1500, 2001.

[18] J. L. Pearlman, S. S. Roach, and F. J. Valero-Cuevas, "The fundamental thumb-tip force vectors produced by the muscles of the thumb," *J. Orthop. Res.*, vol. 22, pp. 306–312, 2004.

[19] F. J. Valero-Cuevas and H. Lipson, "A computational environment to simulate complex tendinous topologies," presented at the 26th Annu. Int. Conf. IEEE EMBS, San Francisco, CA, 2004.

[20] F. J. Valero-Cuevas, "Predictive modulation of muscle coordination pattern magnitude scales fingertip force magnitude over the voluntary range," *J. Neurophysiol.*, vol. 83, pp. 1469–1479, 2000.

[21] H. Lipson, "A relaxation method for simulating the kinematics of compound nonlinear mechanisms," *ASME J. Mech. Des.*, vol. 128, pp. 719–728, 2006.

[22] H. Lipson and J. B. Pollack, "Automatic design and manufacture of robotic lifeforms," *Nature*, vol. 406, pp. 974–978, 2000.

[23] C. Paul, H. Lipson, and F. J. Valero-Cuevas, "Evolutionary form-finding of tensegrity structures," in *Proc. 2005 Genetic and Evolutionary Computation Conf. (GECCO)*, Washington, DC, 2005, pp. 3–10.

[24] M. Garcia-Elias, K. N. An, L. J. Berglund, R. L. Linscheid, W. P. Cooney, and E. Y. Chao, "Extensor mechanism of the fingers: II. Tensile properties of components," *J. Hand Surg. (Am.)*, vol. 16, pp. 1130–1140, 1991.

[25] H. Imamizu, T. Kuroda, S. Miyauchi, T. Yoshioka, and M. Kawato, "Modular organization of internal models of tools in the human cerebellum," *Proc. Nat. Acad. Sci. USA*, vol. 100, pp. 5461–5466, 2003.

[26] A. d'Avella and E. Bizzi, "Shared and specific muscle synergies in natural motor behaviors," *Proc. Nat. Acad. Sci USA*, vol. 102, pp. 3076–3081, 2005.

[27] M. Garcia-Elias, K. N. An, L. Berglund, R. L. Linscheid, W. P. Cooney, and E. Y. Chao, "Extensor mechanism of the fingers: I. A quantitative geometric study," *J. Hand Surg. (Am.)*, vol. 16, pp. 1130–1140, 1991.

[28] Y. Ikebuchi, T. Murakami, and A. Ohtsuka, "The interosseous and lumbrical muscles in the human hand, with special reference to the insertions of the interosseous muscles," *Acta Med. Okayama*, vol. 42, pp. 327–334, 1988.